

CMOS Buck-Boost Power processing circuitry for powerMEMS generators

R. D'hulst^{1*}, P. D. Mitcheson², J. Driesen¹

¹K.U.Leuven - ESAT/ELECTA

Kasteelpark Arenberg 10, B-3001 Heverlee (Belgium)

²Department of Electrical and Electronic Engineering

Imperial College London, Exhibition Road, South Kensington, London, SW7 2AZ

Abstract

This contribution describes a power extraction circuit designed to interface to a vibrational energy harvester. Vibrational energy harvesters produce an AC voltage and therefore a power processing circuit is needed to convert the AC voltage into a DC voltage of an appropriate level for supplying a low power load. The power conversion circuitry must also present the correct electrical impedance to the generator to maximize its power output. The buck-boost topology is chosen for the extraction circuit, its operating point in to discontinuous mode. A reservoir capacitor is present to store the extracted energy. An implementation of the design was simulated using a standard 80 V CMOS process, and efficiencies of over 60% are demonstrated. With suitable control, the input impedance of the circuit is indeed resistive as well as variable and thus well suited as a load for powerMEMS generators.

Keywords: Energy Harvesting, Power Processing circuit, Buck-Boost converter, integrated CMOS

1 - INTRODUCTION

The current trends towards miniaturization, portability and ambient intelligent networks require new means to produce energy in a decentralized fashion. 'Energy harvesters' offer a solution to this problem. These are devices able to convert ambient energy in the environment into useful energy to power, for example, an autonomous sensor. New MEMS techniques are used for fabrication of these micro power generators [1, 2]. The output power of such devices is very limited, ranging from milliwatts down to only a few microwatts. In this paper a power extraction circuit designed to interface to the electrostatic vibrational energy harvester described in [2] is presented, although the circuit may also be applicable to the other vibration-driven generator types (piezoelectric and electromagnetic) [3, 4]. All three types can be modeled as mass-spring-damper systems. When there is relative motion between the mass and the generator housing work is done against the damper and this represents the energy generated.

Vibrational energy harvesters produce an AC voltage and therefore a power processing circuit is needed to convert the AC voltage into a DC voltage of an appropriate level for supplying a low power load. The power density

of an energy harvester (at resonance) increases with the amplitude of the relative motion between the proof mass and generator housing and therefore the power conversion circuitry must also present the correct electrical impedance to the generator to maximize the travel of the proof mass [5].

The input specifications for the power processing circuit are taken as a sinusoidal input voltage with a frequency of 1000 Hz. This is typical for the harvester device in [4] at an energy extraction rate of around 100 μ W. A proposed overall system block diagram is shown in Fig. 1. The first power processing stage must maximize energy extraction from the scavenger mechanics and store it in the reservoir capacitor. The reservoir is present due to the intermittent nature of many vibration sources meaning that the operating duty cycle of the scavenger may be significantly less than 1. The final regulation stage ensures a high quality supply for the load.

2 - BUCK-BOOST CONVERTER

The buck-boost topology [6], shown in Fig. 2, is chosen as the extraction circuit for two main reasons: its simplicity and its ability to step-up and down the voltage. Step up and down is important because as the mechanical operating conditions of the generator change, the voltage

*Contact author: Tel: +32 16 32 10 20, Fax: +32 16 32 19 85, email: reinhilde.dhulst@esat.kuleuven.be

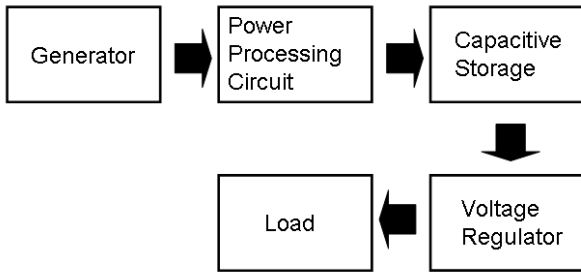


Figure 1 - Energy scavenger system level diagram.

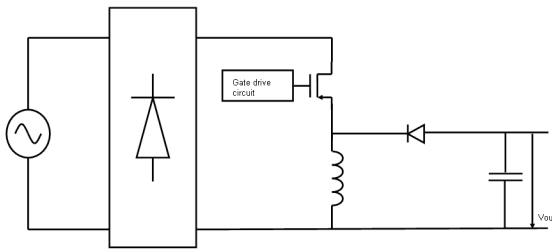


Figure 2 - Basic Buck-Boost AC-DC switch-mode power converter.

at the input to the extraction circuit may fluctuate above and below the voltage on the storage capacitor. The operating point of the buck-boost switching converter is set to discontinuous mode, in order to reduce switching losses, and to keep the inductance as small as possible. This may allow integration of the inductor on chip and will at the very least ensure that external component sizes are minimized [7]. A high voltage is allowed on the output capacitor, to ensure optimal energy capture from the generator at all times, while energy usage by the load is variable. The input current of the buck-boost converter is shown in Fig. 3. The on-time ($T_{on} = DT_s$) of the switch is kept constant, as to assure a 'resistive' input impedance as is required by the scavenger. This load impedance needs to be variable to be able to optimize energy collection at different harvesting conditions. The input impedance of the processing circuit can be easily adapted by changing T_{on} of the main power transistor. Moreover, the input current drawn from the harvester is sinusoidal, this significantly increases energy yield compared to the use of a simple diode rectifier according to [7].

The peak input current can be approximated by eq. (1), if $T_s \ll \frac{1}{f_h}$, with $T_s = \frac{1}{f_s}$ the switching period of the switch, and f_h the input vibration frequency of the scavenger. The output voltage amplitude of the harvester is given by V_I , and the inductance is given by L .

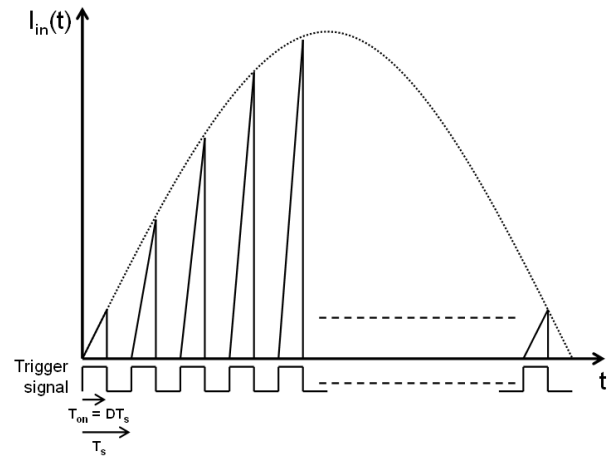


Figure 3 - Input current of the buck-boost converter in discontinuous conduction mode.

$$i_{peak}(t) = \frac{V_I |\sin(2\pi f_h t)| D}{L f_s} \quad (1)$$

The input current of the converter, averaged over one switching period is given by eq. (2).

$$i_{avg}(t) = \frac{V_I |\sin(2\pi f_h t)| D^2}{2L f_s} \quad (2)$$

The average input power of the converter is then given by eq. (3), this equation is used to calculate T_{on} , given a certain input power.

$$P_{in} = 2f_h \int_0^{\frac{1}{2f_h}} \frac{V_I^2 |\sin^2(2\pi f_h t)| D^2}{2L f_s} dt = \frac{D^2 V_I^2}{4L f_s} \quad (3)$$

The input resistance is given by eq. (4).

$$R_{in} = \frac{2L f_s}{D^2} \quad (4)$$

A high switching frequency should be used if a small inductance is desired, to allow for a fully integrated circuit. At very high f_s , T_{on} decreases, but T_{on} should at least be higher than the sum of rise and fall times of the used switch, to allow it to turn fully on. The fall time of the current through the inductance is proportional to i_{peak} , and inversely proportional to the output voltage. To allow for a minimal current fall time at high output voltages, the switching frequency cannot be too high. An inductance of 10 μH is used further on, a PCB-integrated inductor with this inductance seems to be feasible [8]. A switching frequency of 100 kHz is chosen, this gives a theoretical T_{on} of about one order larger than the reported sum of the transistor rise and fall times, with an input voltage range between 1 and 15 V, and an input power range of 10-100 μW . Figure 4 shows how the T_{on} of the switch varies with varying input power and voltage amplitude, it

can be seen that a low input voltage has an advantageous effect on T_{on} . The highest achievable output voltage, allowing for an acceptable current fall time is then about 20 V.

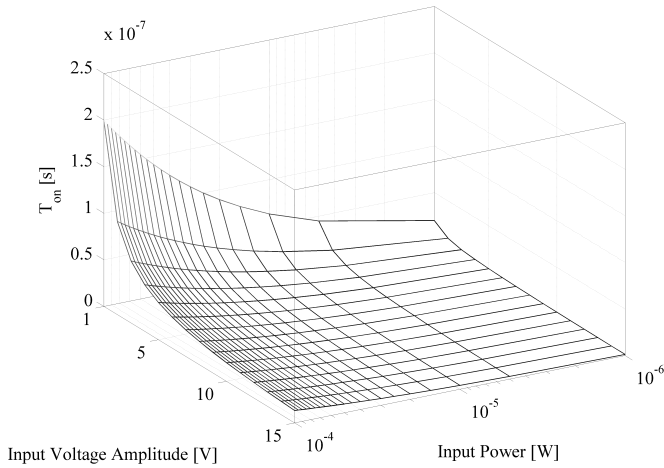


Figure 4 - T_{on} versus P_{in} and V_I .

3 - IMPLEMENTATION

3.1 - Component sizing

The design has been implemented and simulated using a standard 80 V CMOS process. High-voltage diodes and high-voltage transistors are available in this technology. The size of the power transistor was optimized by minimizing gate-charge losses as well as conduction and switching losses. Because conduction times of the transistor are very short, it is hard and even irrelevant to make a distinction between conduction and switching losses. As can be seen from Fig. 5, simply optimizing for conduction losses is not sufficient, gate charge losses are significant, so a compromise has to be made. Still, the gate-charge losses amount to almost one third of the total power transistor losses at the optimal transistor size. A decrease of the gate-charge losses is obtained by purposely under driving the gate with a low turn-on voltage. The threshold voltage of the high-voltage transistors lies at 0.7 V, if a gate drive voltage of 1 V is used in stead of the commonly used 3.3 V, the total loss due to the power transistor can be reduced with 25% at the optimal transistor size, as shown in Fig. 6. Diode losses, including reverse recovery losses, are minimal if the largest available diode area is used.

A diode rectifier is implemented for initial rectification, chosen for its simplicity. Possibly a fully synchronous rectifier is more efficient, to be investigated in future work.

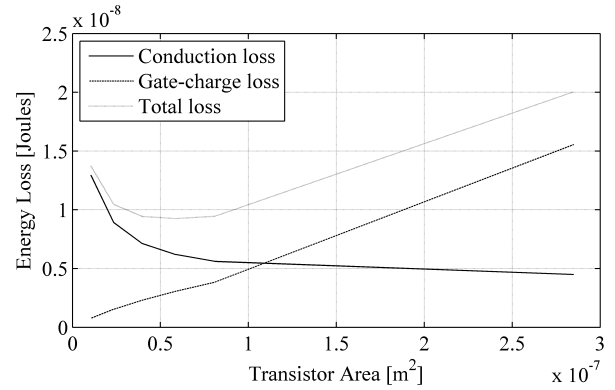


Figure 5 - Conduction loss, gate-charge loss and total power loss during half a vibration period, versus the transistor area.

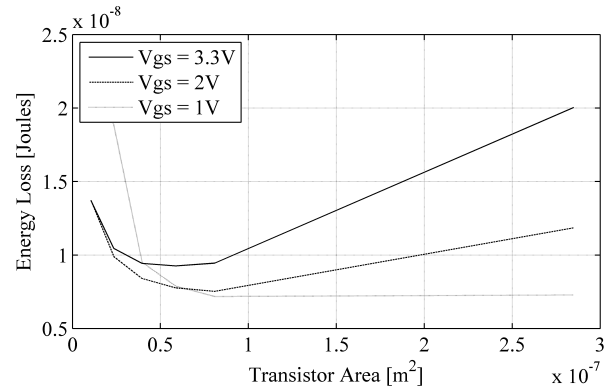


Figure 6 - Total energy loss versus transistor area, at different turn-on voltages.

3.2 - Synchronous rectification

To avoid the power loss due to the forward voltage drop over the diode, a design with synchronous rectification has been implemented. The same conclusions for the sizing of the synchronous rectifying transistor can be drawn concerning gate charge losses and conduction losses of the main switch transistor, versus transistor size. Therefore, both the main switching transistor and the rectifying transistor are chosen to be equal in size and are driven with a gate-drive voltage of 1 V. Simulations show that the total synchronous rectifier losses are substantially less than the diode losses, if the same input power is drawn from the source. Figure 7 shows the distribution of the energy losses of the different components during one scavenger vibration period. 'Eds1' and 'Egc1' are the drain-source and the gate-charge losses of the main switch transistor, 'Edio' are the diode losses, 'Eds2' and 'Egc2' are the losses in the synchronous rectifier and 'Eout' is the fraction of the input energy going to the output capacitor. No parasitic losses in the inductor or the output capacitor are taken into account, neither are the losses due to

the gate-drive circuit and other control units. With the use of synchronous rectification, simulations show that an efficiency of more than 60% can be achieved while converting 100 μ W. Efficiency varies greatly with changing output voltage: if the output voltage is low, the efficiency is low, due to the long conduction times of the diode or the synchronous rectifier transistor. The efficiency gain of synchronous rectification with respect to the use of a diode is higher, because conduction losses of the synchronous rectifier-transistor are lower, see Fig. 7. At higher output voltages the efficiency gain decreases, conduction times become very short, explaining the smaller difference in efficiency between synchronous rectification and the use of a diode. The efficiency decreases at very high output voltages: a very large inductor current fall-rate combined with a finite diode reversing time, causes the current to become negative for a very short time. This reversed current flows back to the generator through the parasitic diode of the main transistor, explaining the lower energy output at the highest voltage in Fig. 7, this effect has to be avoided. The size of the output capacitor is determined by the amount of energy needed to be buffered. This amount depends on the requirements of the load and on the duty-cycle of the harvester. An optimal capacitor size can be derived according to the load and harvester characteristics, to ensure that the output voltage of the converter at most times, is the voltage where the converter works at optimal efficiency.

4 - CONCLUSION

In this contribution a proposal is made for a power processing circuit for vibrational energy harvesters. The circuit has to perform an AC-DC conversion as well as present the correct electrical impedance to the energy harvester to maximise its power output. This is achieved by a buck-boost topology, working in discontinuous conduction mode. The design has been implemented in a 80 V CMOS technology, and proves to have a conversion efficiency of more than 60%. The input impedance is resistive and easily adaptable to different operating conditions.

ACKNOWLEDGEMENTS

Research presented in this paper is financed by the IWT (Institute for Promotion and Innovation by Science and Technology in Flanders) under the project SBO 030288 "PowerMEMS".

REFERENCES

- [1] A. Holmes, G. Hong, K. Pullen, and K. Buffard, "Axial-flow microturbine with electromagnetic generator: design, CFD simulation, and prototype demonstration," in *Micro Electro Mechanical Systems, 2004. 17th IEEE International Conference on. (MEMS)*, 2004, pp. 568–571.
- [2] T. Sterken, P. Fiorini, K. Baert, R. Puers, and G. Borghs, "An electret-based electrostatic μ -generator," in *TRANSDUCERS, Solid-State Sensors, Actuators and Microsystems, 12th International Conference on, 2003*, vol. 2, 2003, pp. 1291–1294.
- [3] N. Ching, H. Wong, W. Li, P. Leong, and Z. Wen, "A laser-micromachined multi-modal resonating power transducer for wireless sensing systems," *Sensors and Actuators A*, vol. 97-98, pp. 685–690, 2002.
- [4] A. Schmitz, T. Sterken, M. Renaud, P. Fiorini, R. Puers, and C. Van Hoof, "Piezoelectric scavengers in mems technology: Fabrication and simulation," in *The 5th International Workshop on Micro and Nanotechnology for Power Generation and Energy Conversion Applications (PowerMEMS 2005)*, University of Tokyo, Japan, Nov.28-30 2005, pp. 61–64.
- [5] P.D.Mitcheson, T.C.Green, and E.M.Yeatman, "Power processing circuits for mems inertial energy scavengers," in *Proc. Design, Test, Integration and Packaging of MEMS/MOEMS Symposium*, Stresa, Italy, Apr. 2006, pp. 332–337.
- [6] N. Mohan, T. M. Undeland, and W. P. Robbins, *Power Electronics: Converters, Applications, and Design. Third edition*. John Wiley & Sons, Inc., 2003.
- [7] G. K. Ottman, H. F. Hofmann, and G. A. Lesieutre, "Optimized piezoelectric energy harvesting circuit using step-down converter in discontinuous conduction mode," *IEEE Transactions on Power Electronics*, vol. 18, pp. 696–703, Mar. 2003.
- [8] M. Ludwig, M. Duffy, T. O'Donnell, P. McCloskey, and S. Mathuna, "PCB integrated inductors for low power DC/DC converter," *IEEE Transactions on Power Electronics*, vol. 18, no. 4, pp. 937–945, July 2003.

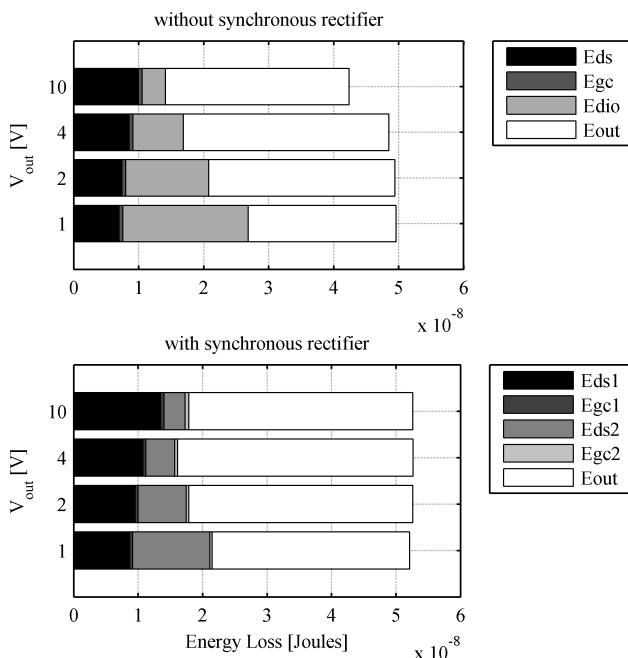


Figure 7 - Distribution of the losses of the different components in the buck-boost converter with and without synchronous rectification, at different output voltages.